Numerical Study for Natural Convection within a Rotating Cubic Enclosure

Dr. Hussein Majeed Salih
Electromechanical Engineering Department, University of Technology /Baghdad
Email:Hussein_maj@yahoo.com

Received on: 4/9/2011 & Accepted on: 3/5/2012

ABSTRACT

A numerical study of three–dimensional, steady, turbulent and incompressible natural convection of air (Pr=0.72) within a rotating cubic enclosure is presented. The present code is based on solving partial differential equations for conservation of mass, momentum and energy equations for a rotating frame. The turbulence effect is introduced by using two equations turbulence model of k-e . Finite volume method is used in solving the governing equations. SIMPLE algorithm is applied to solve the set discretization equations. To verify the validity of present method, present results is compared with those of previous published work under the same conditions. The influence of changing rotation Rayleigh number (Ra_r) as a result of chancing angular velocity of enclosure, and temperature difference of enclosure walls on the average Nusselt number (Nu) is presented and correlated.

Keywords: CFD, Natural convection, rotating enclosure, numerical analysis**.**

دراسة عددية للحمل الحر خلال حيز مكعب دوار

الخلاصة

تم تقديم دراسة عددية ثلاثية الابعاد للحمل الحر المستقر ، المضطرب والغير قابل للانضغاط للهواء الموجود في حيز مكعب مغلق دوار. تم بناء برنامج حسابي لحل المعادلات التفاضلية لحفظ الكتلة والزخم والطاقة للهياكل الدوارة. تم تمثيل الاضطراب بواسطة نموذج الاظطراب ثنائي المعادلات ($k-e$) . استخدمت طريقة الحجوم المحددة في حل المعادلات وطبقت طريقة (SIMPLE) لحل المعدلات. تم التحقق من وثوقية البرنامج المعد في هذه الدراسة بواسطة مقارنة نتائجه مع نتائج بحث منشور سابقاً عند نفس الظروف. تم دراسة تاثير تغيير قيمة عدد رايلي للدوران نتيجة تغيير قيمة السرعة الدورانية للحيز وكذلك تغيير قيمة فرق درجات الحرارة لجدران الحيز على قيمة معدل عدد نسلت (Nu) وكذلك تم ايجاد علاقة رياضة تربط بين عدد رايلي للدوران ومعدل عدد نسلت.

PDF created with pdfFactory Pro trial version www.pdffactory.com

V^*	dimensionless vertical velocity component $\left(v/\sqrt{gb\Delta TL}\right)$
w	velocity component in z direction (m/s)
x	coordinate (m)
y	coordinate (m)
z	coordinate (m)

Greek symbols

a	thermat diffusivity (m^2/s).
b	volumetric coefficient of thermal expansion (K^{-1})
Φ	dependent variable used in discretization equation.
Γ_Φ	diffusion coefficient used in discretization equation.
m	dynamic viscosity (kg/m s)
n	kinematic viscosity (m^2/s)
r	density of the fluid (kg/m^3)
ΔT	wall temperature difference (T_H-T_C).

Subscripts

C	cold
eff	effective
H	hot
t	turbulence

Nomenclature

A	coefficient for the discretization equation
c_p	specific heat ($J/kg.K^o$)
c_{e1}, c_{e2}, c_m	constants in the k-e equation
f	under relaxation factor
G_k	turbulent production term
g	gravitational acceleration (m/s^2)
k	turbulent kinetic energy
L	length of enclosure (m)
Nu	average Nusselt number
P	pressure (N/m^2)
Pr	Prandtl number (n/a)
Ra	Rayleigh number $\left(\frac{gb\Delta TS^3}{an}\right)$
Ra_r	rotation Rayleigh number $\left(\frac{b\Omega^2 r\Delta TL^3}{an}\right)$
r	radius of rotation of enclosure (m)
S	source term
T	temperature (K)
u	velocity component in x direction (m/s)
v	velocity component in y direction (m/s).

INTRODUCTION

The rotating flow is one of the most challenging research fields of fluid mechanics. Rotating electronics cooling can be encountered in some rotary machines, the guided missiles and space-based manufacturing process. However, most early works were focused on experimental study with the simple geometries.

Bajaj et al. [1], presented an experimental results for Rayleigh-Bénard convection with rotation about a vertical axis at dimensionless rotation rates $0 \le \Omega \le 250$. While Pino et al. [2] presented a numerical analysis for fluid contained in a fast rotating cylindrical annulus with slightly inclined plane. Vargas et al. [3], described the mechanical characteristics of the centrifuge and its instrumentation. A centrifuge for the study of fluid mechanics phenomena in a rotating frame had been constructed at the Centre of Energy Research at the National

PDF created with pdfFactory Pro trial version www.pdffactory.com

University of Mexico (UNAM). A three-dimensional numerical and asymptotic study of the steady laminar flow driven by a rotating lid at the top of an enclosed cylinder filled with a liquid metal and submitted to an axial magnetic B, was presented by Bessaih and Soudani [4] . The heating of containerized liquid using microwave radiation was investigated numerically and by Chatterjee et al. [5].

On the other hand Scheel [6] derived the amplitude equation for rotating Rayleigh–Bénard convection from the Boussinesq equations with the Coriolis force included. The vertical boundary conditions were no-slip, and the lateral boundary conditions were either periodic or rigid. A numerical simulation of the turbulent natural convection in a square cavity was investigated by Bouaraour [7]. The turbulence was modeled by the low Reynolds number k-e model.

The equations controlling the flow were discretized using the finite volume method. The SIMPLER algorithm was used for the pressure-velocity coupling. The natural convection in an incompressible viscous fluid owing near a semi-infinite impermeable vertical plate had been investigated by Chandran et al., [8]. Assuming that the fluid-plate system was undergoing a rigid-body rotation. The steady free convective flow and mass transfer of a rotating elastic-viscous electrically conducting fluid through a porous medium occupying a semi infinite region of space bounded by an infinite vertical porous plate in presence of a transverse magnetic field with constant suction and heat flux was considered by Das et al., [9]. A Cartesian co-ordinate system rotating uniformly with the fluid in a rigid state of rotation with a constant angular velocity Ω about z-axis was chosen. While, the unsteady free-convection flow of a viscous, heat conducting fluid near an infinite, inclined and rotating plate (or surface) was investigated by Toki [10]. Muthucumaraswamy et al., [11] presented an exact analysis of rotation effects on unsteady flow of an incompressible and electrically conducting fluid past a uniformly accelerated infinite isothermal vertical plate, under the action of transversely applied magnetic field. Theoretical study of thermal radiation effects on unsteady free convective flow over a moving vertical plate in a rotating fluid was considered by Vijayalakshmi [12]. The effects of rotation, radiation, free-convection parameters and the skin friction components on the plate were discussed. Chauhan and Rastogi [13] investigated the unsteady natural convection MHD flow of a rotating viscous electrically conducting fluid in a vertical channel partially filled by a porous medium with high porosity in the presence of radiation effects.

Now, in the present steady the effect of rotation of enclosure on a natural convection within it is investigated. A steady three-dimensional, incompressible momentum and energy equation for turbulent flow for a rotating frame is presented. Finite volume method is used with staggered grid arrangement. The results have been obtained for Prandtl number of 0.72. The effect of change of angular velocity (Ω) and so the rotation Rayleigh number (Ra_r) of the enclosure rotated about the vertical axis (y-axis) on the average Nussult number (Nu) is investigated and correlated.

PDF created with pdfFactory Pro trial version www.pdffactory.com

Problem Definition

A schematic of the physical situation to be investigated is a cubic enclosure which is shown in Figure (1). The vertical walls located at x = 0 and x = L are isothermal at different temperatures of T_H and T_C (left and right) respectively. The upper and lower walls are insulated at y = 0 and y = L, z=0 and z=L. The enclosure rotates about the y-axis counterclockwise with a radius of rotation equal to L/2. The fluid within the enclosure is an air (Pr=0.72).

Governing Equations

The flow in the enclosure is assumed to be steady incompressible three dimensional turbulent. The turbulent flow for the rotating frame is described by the continuity, momentum and energy equations as follow [14]:

Continuity:

$$\frac{\partial(ru)}{\partial x}+\frac{\partial(rv)}{\partial y}+\frac{\partial(rw)}{\partial z}=0 \qquad (1)$$

x-direction momentum equation

$$\frac{\partial(ruu)}{\partial x}+\frac{\partial(rvu)}{\partial y}+\frac{\partial(rwu)}{\partial z}=\frac{\partial}{\partial x}\left[m_{eff}\left(\frac{\partial u}{\partial x}\right)\right]+\frac{\partial}{\partial y}\left[m_{eff}\left(\frac{\partial u}{\partial y}\right)\right]+\frac{\partial}{\partial z}\left[m_{eff}\left(\frac{\partial u}{\partial z}\right)\right]+S_u \qquad (2)$$

y-direction momentum equation

$$\frac{\partial(ruv)}{\partial x}+\frac{\partial(rvv)}{\partial y}+\frac{\partial(rwv)}{\partial z}=\frac{\partial}{\partial x}\left[m_{eff}\left(\frac{\partial v}{\partial x}\right)\right]+\frac{\partial}{\partial y}\left[m_{eff}\left(\frac{\partial v}{\partial y}\right)\right]+\frac{\partial}{\partial z}\left[m_{eff}\left(\frac{\partial v}{\partial z}\right)\right]+S_v \qquad (3)$$

z-direction momentum equation

$$\frac{\partial(ruw)}{\partial x}+\frac{\partial(rvw)}{\partial y}+\frac{\partial(rww)}{\partial z}=\frac{\partial}{\partial x}\left[m\left(\frac{\partial w}{\partial x}\right)\right]+\frac{\partial}{\partial y}\left[m\left(\frac{\partial w}{\partial y}\right)\right]+\frac{\partial}{\partial z}\left[m_{eff}\left(\frac{\partial w}{\partial z}\right)\right]+S_w \qquad (4)$$

Energy:

PDF created with pdfFactory Pro trial version www.pdffactory.com

$$\frac{\partial(ruT)}{\partial x}+\frac{\partial(rvT)}{\partial y}+\frac{\partial(rwT)}{\partial z}=\frac{\partial}{\partial x}\left[\Gamma_{eff}\left(\frac{\partial T}{\partial x}\right)\right]+\frac{\partial}{\partial y}\left[\Gamma_{eff}\left(\frac{\partial T}{\partial y}\right)\right]+\frac{\partial}{\partial z}\left[\Gamma_{eff}\left(\frac{\partial T}{\partial z}\right)\right]+S_T \quad (5)$$

The value of m_{eff} in equations (2,3 and 4) is

$$m_{eff}=m+m_t \quad (6)$$

and

$$S_u=-\frac{\partial P}{\partial x}+\frac{\partial}{\partial x}\left[m_{eff}\left(\frac{\partial u}{\partial x}\right)\right]+\frac{\partial}{\partial y}\left[m_{eff}\left(\frac{\partial v}{\partial x}\right)\right]+\frac{\partial}{\partial z}\left[m_{eff}\left(\frac{\partial w}{\partial x}\right)\right]+r\Omega(\Omega.x-2w) \quad (7)$$

$$S_v=-\frac{\partial P}{\partial y}+\frac{\partial}{\partial x}\left[m_{eff}\left(\frac{\partial u}{\partial y}\right)\right]+\frac{\partial}{\partial y}\left[m_{eff}\left(\frac{\partial v}{\partial y}\right)\right]+\frac{\partial}{\partial z}\left[m_{eff}\left(\frac{\partial w}{\partial y}\right)\right]+rgb(T-T_c) \quad (8)$$

$$S_w=-\frac{\partial P}{\partial x}+\frac{\partial}{\partial x}\left[m_{eff}\left(\frac{\partial u}{\partial z}\right)\right]+\frac{\partial}{\partial y}\left[m_{eff}\left(\frac{\partial v}{\partial z}\right)\right]+\frac{\partial}{\partial z}\left[m_{eff}\left(\frac{\partial w}{\partial z}\right)\right]+r\Omega(\Omega.z+2u) \quad (9)$$

$$\Gamma_{eff}=\frac{m}{Pr}+\frac{m_t}{Pr_t} \quad (10)$$

In thermal energy equation the radiation heat transfer, the viscous dissipation, pressure work and Joule heating are ignored, so the source term S_T becomes

$$S_T=0 \quad (11)$$

m_t: is the turbulent eddy viscosity and estimated by the $k-e$ two-equation turbulence model:

PDF created with pdfFactory Pro trial version www.pdffactory.com

$$m_t = \frac{c_m r k^2}{e} \tag{12}$$

TURBULENCE MODELING

Turbulence closure was provided by means of a non-linear eddy-viscosity model. Whilst this model cannot exactly represent the modifications to the turbulence production rate due to Coriolis and centripetal forces (these contributions have zero trace), the model is able to give some representation of normal-stress anisotropy, streamline curvature and bulk rotation effects. The model consists of transport equations for k and e and an expansion for the anisotropy tensor involving terms up to, and including those, cubic in the mean strain and vorticity tensors. The turbulent transport equations are as follows:

Turbulence energy , k

$$\frac{\partial(ruk)}{\partial x}+\frac{\partial(rvk)}{\partial y}+\frac{\partial(rwk)}{\partial z}=\frac{\partial}{\partial x}\left[\Gamma_k\left(\frac{\partial k}{\partial x}\right)\right]+\frac{\partial}{\partial y}\left[\Gamma_k\left(\frac{\partial k}{\partial y}\right)\right]+\frac{\partial}{\partial z}\left[\Gamma_k\left(\frac{\partial k}{\partial z}\right)\right]+G_k-re \tag{13}$$

Dissipation rate, e

$$\frac{\partial(rue)}{\partial x}+\frac{\partial(rve)}{\partial y}+\frac{\partial(rwe)}{\partial z}=\frac{\partial}{\partial x}\left[\Gamma_e\left(\frac{\partial e}{\partial x}\right)\right]+\frac{\partial}{\partial y}\left[\Gamma_e\left(\frac{\partial e}{\partial y}\right)\right]+\frac{\partial}{\partial z}\left[\Gamma_e\left(\frac{\partial e}{\partial z}\right)\right]+C_{e1}G_k\frac{e}{k}-C_{e2}r\frac{e^2}{k} \tag{14}$$

Where

$$\Gamma_k = m+\frac{m_t}{s_k}\ ,\ \Gamma_e = m+\frac{m_t}{s_e} \tag{15}$$

and the turbulent production term is

$$G_k = m_t\left[2\left(\left(\frac{\partial u}{\partial x}\right)^2+\left(\frac{\partial v}{\partial y}\right)^2+\left(\frac{\partial w}{\partial z}\right)^2\right)+\left(\frac{\partial u}{\partial x}+\frac{\partial v}{\partial y}+\frac{\partial w}{\partial z}\right)^2\right] \tag{16}$$

PDF created with pdfFactory Pro trial version www.pdffactory.com

The last coefficients appearing in equation (7) are the same as those adopted in ref. [15] in the standard $k-e$ two-equation turbulence model. These coefficients are:

$$c_m = 0.09,\ s_k = 1.0\ ,\ s_e = 1.3,\ C_{e1} = 1.44\ ,\ C_{e2} = 1.92$$

BOUNDARY CONDITIONS

The boundary conditions to be satisfied for the problem are expressed as:

- At the left wall x=0, $0 < y < L$, $0 < z < L$, $u=0, v=0, w=0, T=T_H$

- At the right wall x=L, $0 < y < L$, $0 < z < L$, $u=0, v=0, w=0, T=T_C$.

- At the bottom wall y=0, $0 < x < L$, $0 < z < L$, $u=0, v=0, w=0, \dfrac{\partial T}{\partial y} = 0$.

- At the top wall y=L, $0 < x < L$ $u=0$, $0 < z < L$, $v=0, w=0, \dfrac{\partial T}{\partial y} = 0$.

- At the front wall z=0, $0 < x < L$, $0 < y < L$, $u=0, v=0, w=0, \dfrac{\partial T}{\partial z} = 0$.

- At the back wall z=L, $0 < x < L$, $0 < y < L$, $u=0, v=0, w=0, \dfrac{\partial T}{\partial z} = 0$.

NUSSELT NUMBER

One of the characteristic of flow is the rate of heat transfer across the cavity. The local Nusselt number at the hot wall is calculated as :

1. $$Nu\big|_{x=0} = \frac{\partial T}{\partial x}\frac{L}{(T_H - T_C)} \qquad (17)$$

While the average Nusselt number at the hot wall is given by:

$$\overline{Nu} = \int_0^{y=L}\left(\frac{\partial T}{\partial x}\right)dy\Big|_{x=0} \qquad (18)$$

METHOD OF SOLUTION

The SIMPLE algorithm by Patankar and Spalding [16] is applied to solve the conservation equation of mass, momentum and energy. The transport equations for continuity equation, momentum equation, energy equation, turbulence energy equation and dissipation rate equation all have the general form in three dimensional geometry:

PDF created with pdfFactory Pro trial version www.pdffactory.com

$$\frac{\partial(ru\Phi)}{\partial x}+\frac{\partial(rv\Phi)}{\partial y}+\frac{\partial(rw\Phi)}{\partial z}=\frac{\partial}{\partial x}\left[\Gamma_\Phi\left(\frac{\partial\Phi}{\partial x}\right)\right]+\frac{\partial}{\partial y}\left[\Gamma_\Phi\left(\frac{\partial\Phi}{\partial y}\right)\right]+\frac{\partial}{\partial z}\left[\Gamma_\Phi\left(\frac{\partial\Phi}{\partial z}\right)\right]+S_\Phi \quad (19)$$

Equation (8) is re-arrangement of algebraic equation of the form:

$$(A_i - S_P)\Phi_P = \sum_{nb} A_i\Phi_i + S_u \quad (20)$$

The set of finite volume equations is solved by using an iteration method, starting from the solution of a previous run as initial condition. Numerical stability is enhanced by the choice of approximate relaxation factor f defined as:

$$\Phi_P^n = f\ \Phi_P + (1-f)\Phi_P^o \quad (21)$$

Where, Φ_P^o is the value of Φ from the previous iteration, Φ_P is the values obtained from the solved equation (9) and Φ_P^n is the new value. The value of the relaxation factor f can be in the range of $0 < f \le 1$.

Grid Arrangement

The special arrangement used for the grid nodes (non-uniform spacing) gives good results even for relatively coarse grids. Fig.1b shows the mesh distributed for the enclosure. There are three sets of grid with clustering near the hot and cold wall are tested, where (60*20*10) is chosen because this set ensure good results and time saving as shown in Fig.1c which represents grid independency, where the vertical velocity component (v) calculated at the mid-height of the enclosure for Ra = $1.5*10^{10}$.

Validity Of Present Code

In order to verify the accuracy of the present numerical investigation obtained from the developed computer code which is written in FORTRAN 90, the results of the developed code are compared with the previously published works of Bouaraour [7] under the same conditions for $\left(Ra = 1.58*10^9\right)$. As can be seen from Fig.2, the present code provides good results.

PDF created with pdfFactory Pro trial version www.pdffactory.com

RESULTS AND DISCUSSION

The focal point of this work is to investigate the relation between average Nusselt number (Nu) and the rotation Rayleigh number (Ra_r) and then predict the correlation for this relation. Thus, the results will be summarized as flow:

Variation Of Angular Velocity With Constant Temperature Difference

Consider the solution for ($\Omega = 0,10,20,30, \; and \; 40$) rad/s and constant temperature difference ($\Delta T = 200$). From the results, the velocity vector has the same behavior for each case except there is an increase in the magnitude of velocity with increasing (Ω). According to this it will consider one of these cases to compare it with the zero rotation ($\Omega = 0$) , this case let to be ($\Omega = 40$) rad/s. Figure (3) illustrate the velocity vector for ($\Omega = 0, \; and \; 40$) rad/s. From Figure (3a), the effect of rotation of the enclosure is seen from the clockwise rotation of flow within the enclosure (opposite to the direction of enclosure rotation) as a result of the pressure variation across the enclosure and the formation of pressure and suction sides in the leading and trailing edges of the enclosure respectively, with addition to the effect of centrifugal and Coriolis forces.

Figure (3b) represents the velocity vector for stationary enclosure. It can be seen that the velocity of flow is effected by the bouncy force as a result of temperature variation of the enclosure walls.

Figure (4) illustrates the temperature contour for the cases ($\Omega = 0,10,20,30, \; and \; 40$) rad/s with also constant temperature difference ($\Delta T = 200$). From these figures, it can be seen that the warm area increased with increasing the angular velocity of the enclosure. Whereas the variation of temperature in the stationary enclosure is increased gradually upward as a result of the effect of bouncy force.

Figure (6) shows the local Nusselt number at the hot wall for the same conditions as in the previous figures. It can be noted that there is an increase in the (Nu) with increasing (Ω) as a result of the centrifugal force and the value of (Nu) is maximum near the lower surface as a result of acceleration of convection currents. In addition to this there is a noticeable increase in the (Nu) near the upper surface with contrast with those for stationary enclosure ($0\,\Omega$) as a result of the vortices formation inside the enclosure which rotate in an opposite direction to those enclosure.

Variation In Temperature Difference With Constant Angular Velocity

Figure (5) represents temperature contour for ($\Delta T = 100,200,300, \; and \; 400$) with constant angular velocity $(\Omega = 50 \, rad/s)$. From these figures the shape of temperature distribution within the enclosure is the same for each case, while the magnitude of temperature increased with increasing temperature difference.

Figure (7) shows the local Nusselt number at the hot wall for the same conditions of Figure (5). From these figures, there is no notable change in the (Nu) and the Nusselt number distribution is the same for these cases. According to this one can conclude that Nusselt number influenced significantly by rotation.

Finally, from all these cases, Figure (8) illustrates the relation between average Nusselt number with rotation Rayleigh number (Ra_r). From this figure, average

PDF created with pdfFactory Pro trial version www.pdffactory.com

Nusselt number is increasing with the rotation Rayleigh number increasing. With the aid of this figure, average Nusselt number can be correlated in terms of (Ra_r). The correlation can be presented by the equation of form:

$$Nu = m(Ra_r)^n \tag{22}$$

Employing the least square technique, the correlation equation is as:

$$Nu = 0.119(Ra_r)^{0.17747} \tag{23}$$

CONCLUSIONS

A numerical study of three –dimensional, steady and incompressible turbulent natural convection of air (Pr=0.72) within a rotated cubic enclosure is presented. Finite volume with staggered grid arrangement is used to solve the governing equations. The two equation turbulence model of k-e is used to introduce the effect of turbulence. The results show that the turbulence increased with increasing the angular velocity of the enclosure and as a result of this there is an increase in the average Nusselt number at the hot wall. The effect of changing rotated Rayleigh number as a result of chancing angular velocity of enclosure, and temperature difference of enclosure walls on the average Nusselt number (Nu) is presented and correlated.

FUTURE WORK

This work can be developed by studying the following:

1. Effect of changing the fluid within the enclosure on the results.
2. Effect of radius of rotation on the nature of flow within the enclosure.
3. Change the direction of rotation for the enclosure (rotated about x-axis or z-axis).

REFERENCES

[1]. Kapil M. S. Bajaj, Jun Liu, Brian Naberhuis, and Guenter Ahlers " Square Patterns in Rayleigh-Bénard Convection with Rotation about a Vertical Axis" The American Physical Society, Physical Review Letters, Vol.81, No. 4, July 1998.

[2].David Pino, Isabel Mercader, and Marta Net " Thermal and inertial modes of convection in a rapidly rotating annulus" The American Physical Society, Physical Review Letters, Vol.61, No. 2, February 2000.

[3]. Vargas,M. E. Ramos, G. Ascanio and R. Espejel, " A Centrifuge for Studies of Fluid Dynamics Phenomena in a Rotating Frame of Reference" Revista Mexicana De Fisica (48),255-266, 2000.

PDF created with pdfFactory Pro trial version www.pdffactory.com

[4].Rachid Bessaih and , Azeddine Soudani " Numerical Simulation of Rotating MHD Flow With Heat Transfer" 12èmes Journées Internationales de Thermique, 2005.

[5]. Sourav Chatterjee , Tanmay Basak and Sarit K. Das "Microwave driven convection in a rotating cylindrical cavity: A numerical study" Indian Institute of Technology, Madras, 2005.

[6]. Scheel " J. D. The amplitude equation for rotating Rayleigh–Bénard convection" American Institute of Physics, Phys. Fluids 19, 104105 , 2007.

[7]. K. Bouaraour " Numerical investigation of natural convection in a square cavity" Journal of Engineering and Applied Science 271-278, 2008.

[8]. Pallath Chandran, Nirmal C Sacheti and Ashok K. Singh " Transient Natural Convection near a Semi-Infinite Vertical Wall in a Rotating System" Differential Equations and Control Processes, Electronic Journal, № 4, 2009.

[9]. S.S. Das, J. P. Panda and A. B. Patnaik " Effect of free convection and mass transfer on MHD flow of a rotating elastico-viscous fluid past an infinite vertical porous plate through a porous medium with constant suction and heat flux" Indian Journal of Science and Technology, Vol.2 No. 9 , Sep. 2009.

[10].C. J. Toki " An Analytical Solution for the Unsteady Free Convection Flow near an Inclined Plate in a Rotating System " Differential Equations and Control Processes, Electronic Journal, № 3, 2009.

[11]. R.Muthucumaraswamy , Tina Lal and D.Ranganayakulu " Effects of rotation on MHD flow past an accelerated isothermal vertical plate with heat and mass diffusion" Theoret. Appl. Mech., Vol.37, No.3, pp. 189–202, Belgrade 2010.

[12]. A.R. Vijayalakshmi " Radiation effects on free-convection flow past an impulsively started vertical plate in a rotating fluid" Theoret. Appl. Mech., Vol.37, No.2, pp. 79{95, Belgrade 2010.

[13]. Chauhan and P. Rastogi, D. S. " Radiation Effects on Natural Convection MHD Flow in a Rotating Vertical Porous Channel Partially Filled with a Porous Medium" Applied Mathematical Sciences, Vol. 4, 2010.

[14]. Nilsson, H., " Numerical investigations of turbulent flow in water turbines." A Ph.D. thesis submitted to the Chalmers University of Technology, Gotebarg, Sweden, 2002.

[15]. Wang, Y., and Komori, S., " Prediction of duct flows with a pressure-based procedure.", Numerical Heat transfer, Part A, 33: 723-748, 1998.

[16]. Patankar, S.V. and Spalding, D.B., " A calculation procedure for heat, mass and momentum transfer in three-dimensional parabolic flows." Int. J. Heat Mass Transfer , Vol. 3, 269-289, 1974.

PDF created with pdfFactory Pro trial version www.pdffactory.com

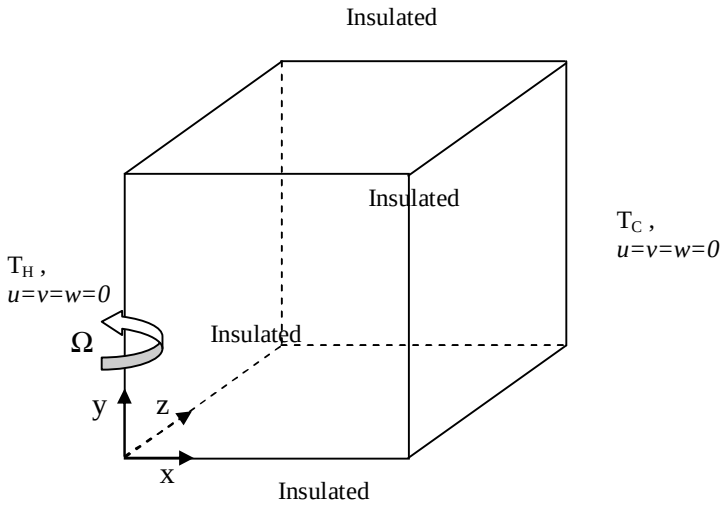


Figure (1a) Geometry and boundary conditions of the problem.

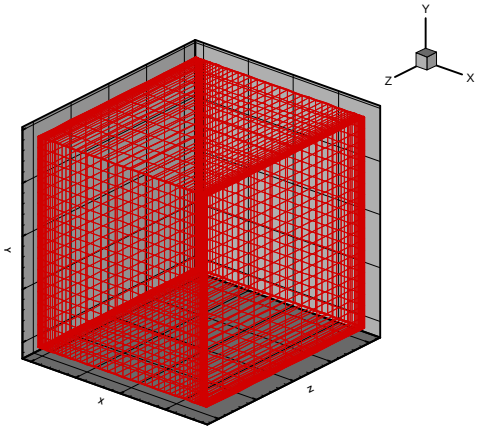


Figure (1b) Grid arrangement

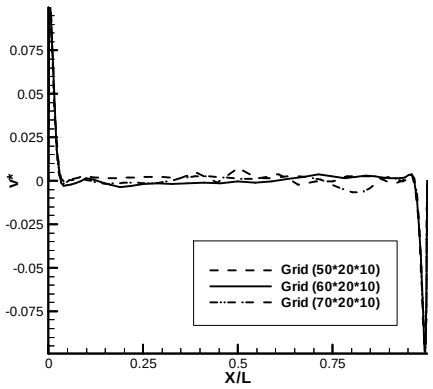


Figure (1c) Grid dependency.

PDF created with pdfFactory Pro trial version www.pdffactory.com

(a) (b)

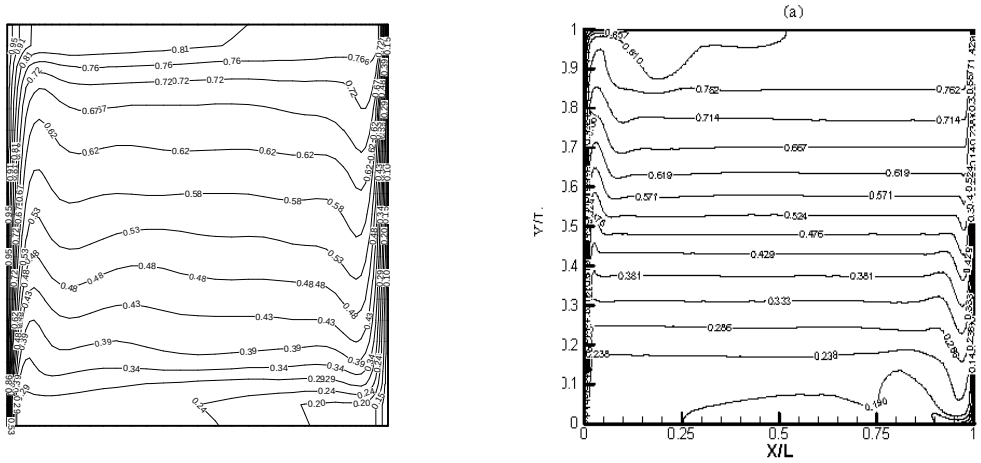
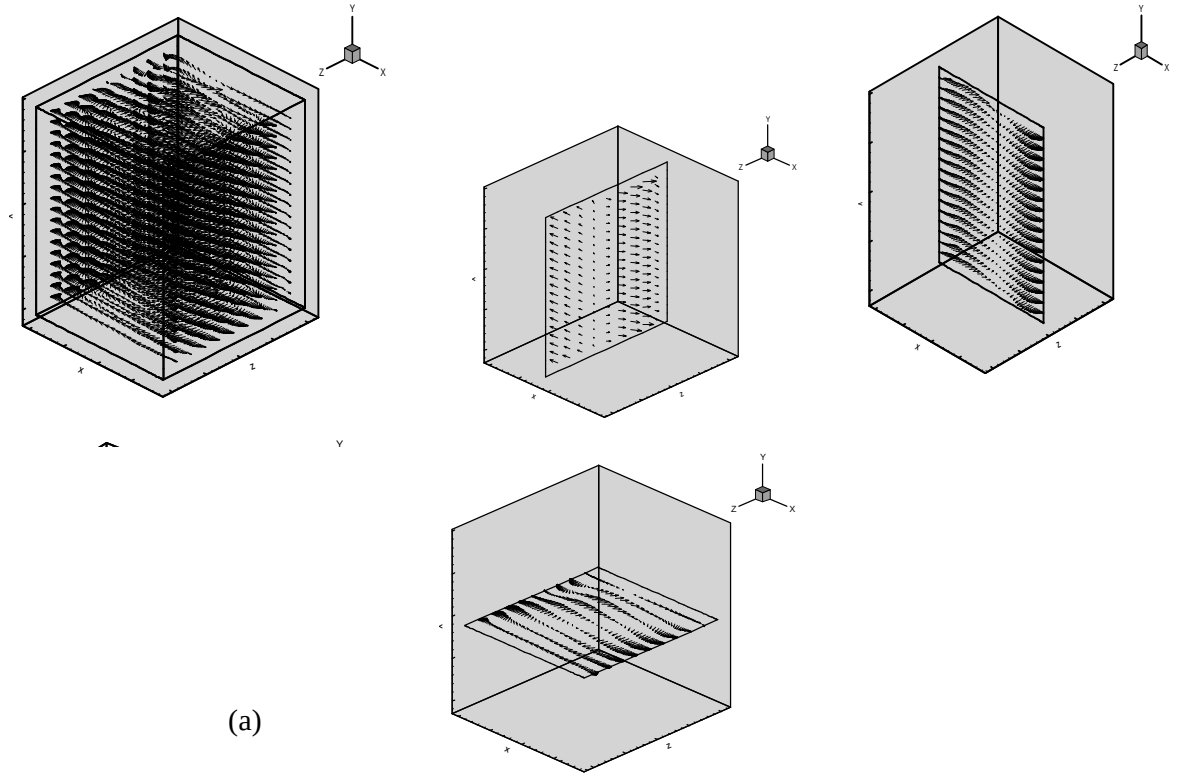
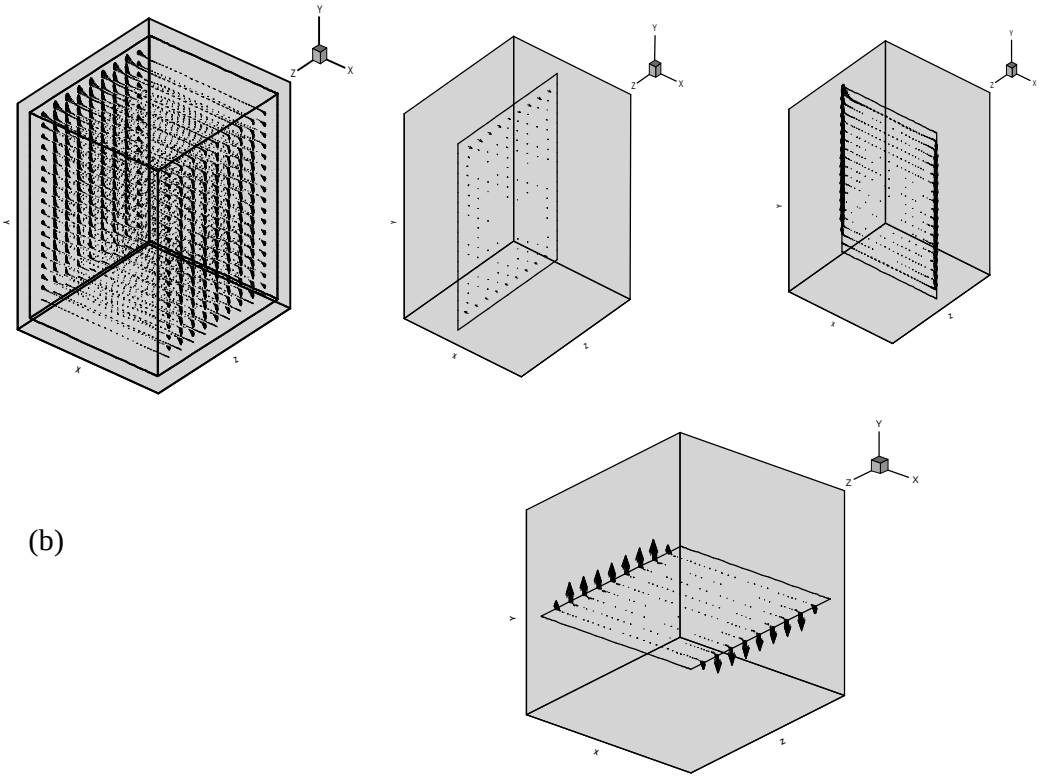


Figure (2) Comparison of the temperature contours for (a) present numerical results, (b) previous work by Bouaraour[7] with $\left(Ra = 1.58 * 10^{9}\right)$.



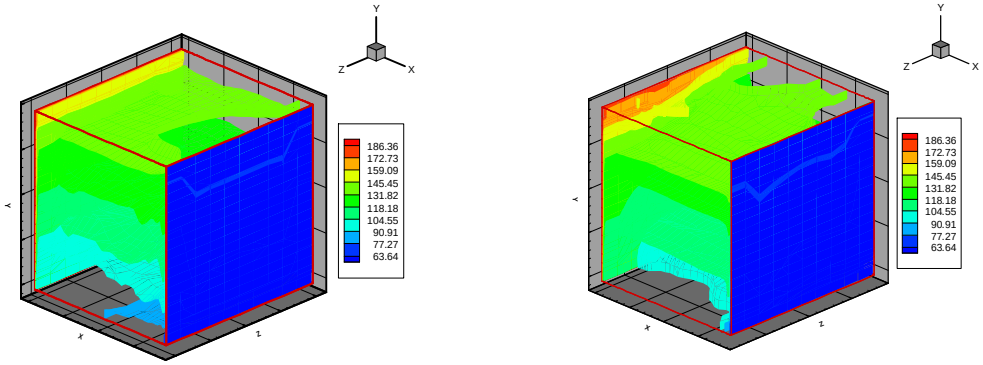
(a)

PDF created with pdfFactory Pro trial version www.pdffactory.com



(b)

Figure (3) Velocity vector: (a) Ω =20 rad/s, Ra=1.67*10^{10}, Ra$_r$=6.47*10^{11}, scale=0.1 relative to grid units/magnitude, (b) Ω =0, Ra=1.67*10^{10}, scale=0.2 relative to grid units/magnitude.



(a) (b)

PDF created with pdfFactory Pro trial version www.pdffactory.com

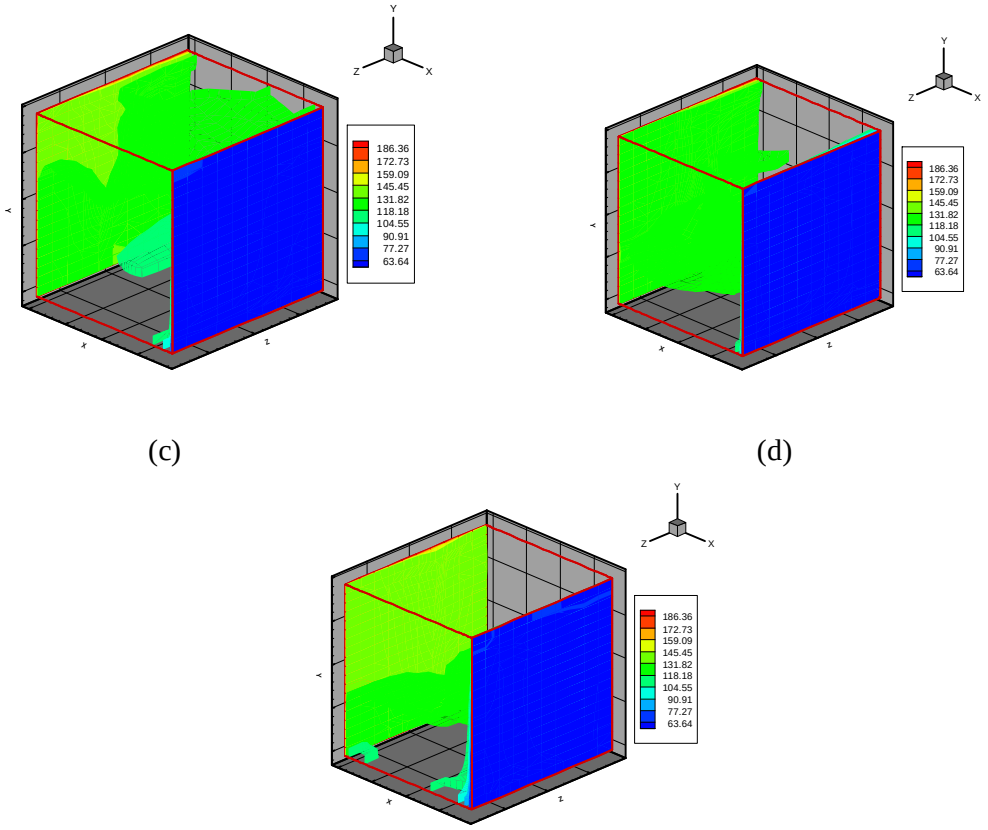


Figure (4) Temperature contour Ra=1.67*10^8, $\Delta T = 150$: (a) Ω =0, (b) Ω =10 rad/s, $Ra_r = 1.6*10^9$, (c) Ω =20 rad/s, $Ra_r = 6.47*10^9$, (d) Ω =30 rad/s, $Ra_r = 1.46*10^{10}$, (e) Ω =40 rad/s, $Ra_r = 2.59*10^{10}$.

PDF created with pdfFactory Pro trial version www.pdffactory.com

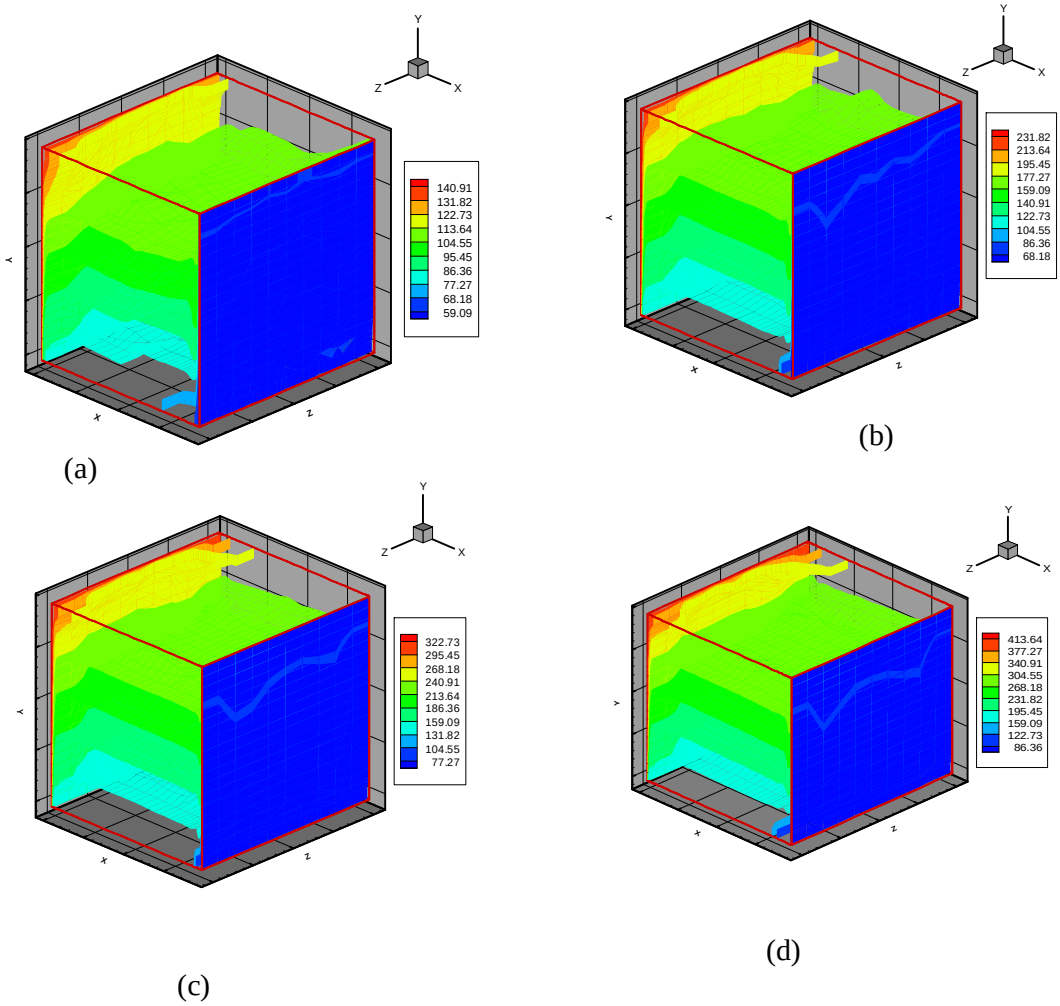


Figure (5) Temperature contour, Ω =50 rad/s: (a) $\Delta T = 100$ **, Ra=1.19**$*10^8$ **,** $Ra_r = 2.88*10^{10}$ **(b)** $\Delta T = 200$ **, Ra=2.09**$*10^8$ **,** $Ra_r = 5.08*10^{10}$ **(c)** $\Delta T = 300$ **, Ra=2.81**$*10^8$ **,** $Ra_r = 6.81*10^{10}$ **(d)** $\Delta T = 400$ **, Ra=3.39**$*10^8$ **,** $Ra_r = 8.21*10^{10}$ **.**

PDF created with pdfFactory Pro trial version www.pdffactory.com

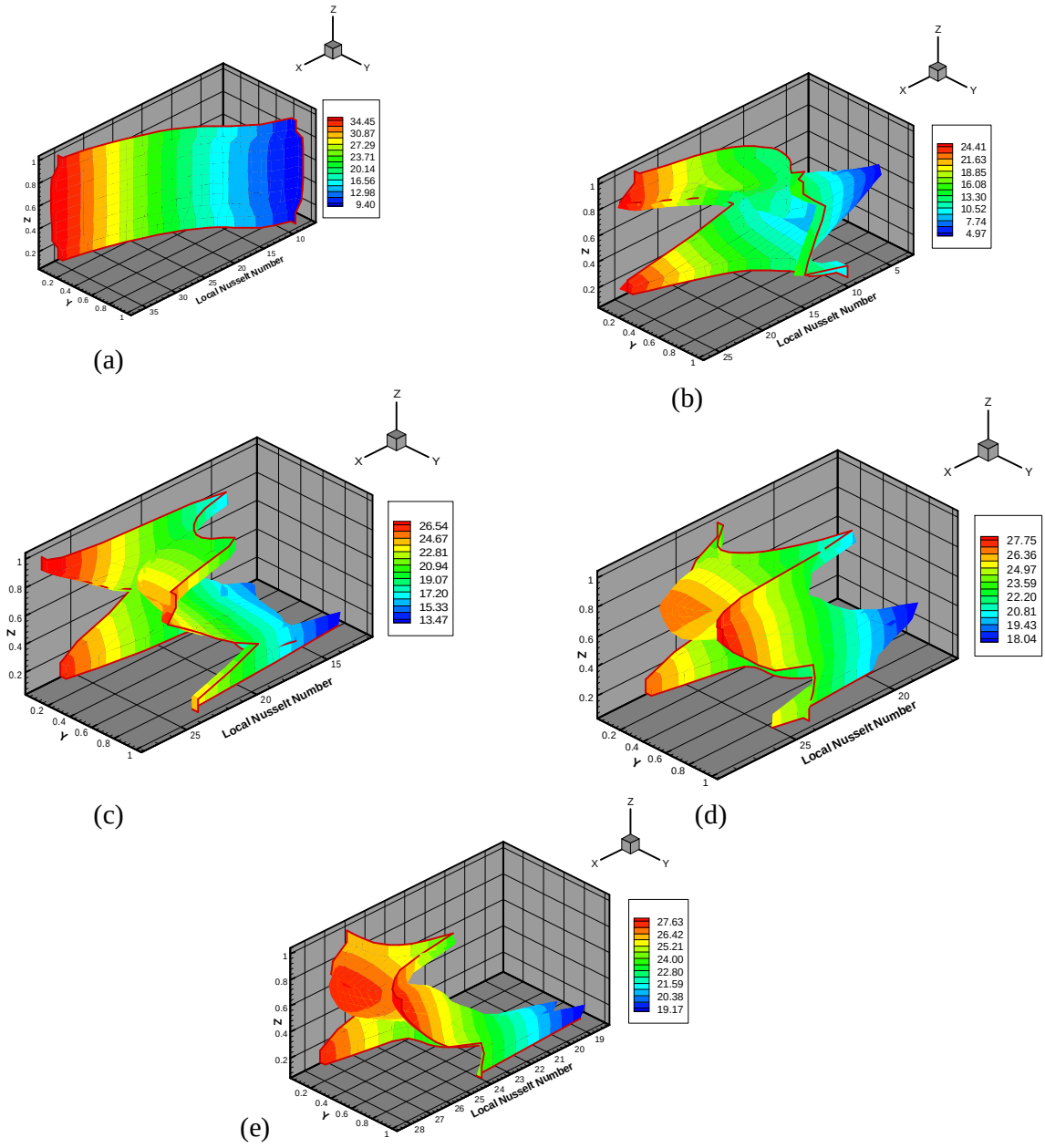


Figure (6) Local Nu contour for hot wall Ra=1.67*10^8, $\Delta T = 150$: (a) Ω=0, (b) Ω=10 rad/s, $Ra_r = 1.6*10^9$, (c) Ω=20 rad/s, $Ra_r = 6.47*10^9$, (d) Ω=30 rad/s, $Ra_r = 1.46*10^{10}$, (e) Ω=40 rad/s, $Ra_r = 2.59*10^{10}$.

PDF created with pdfFactory Pro trial version www.pdffactory.com

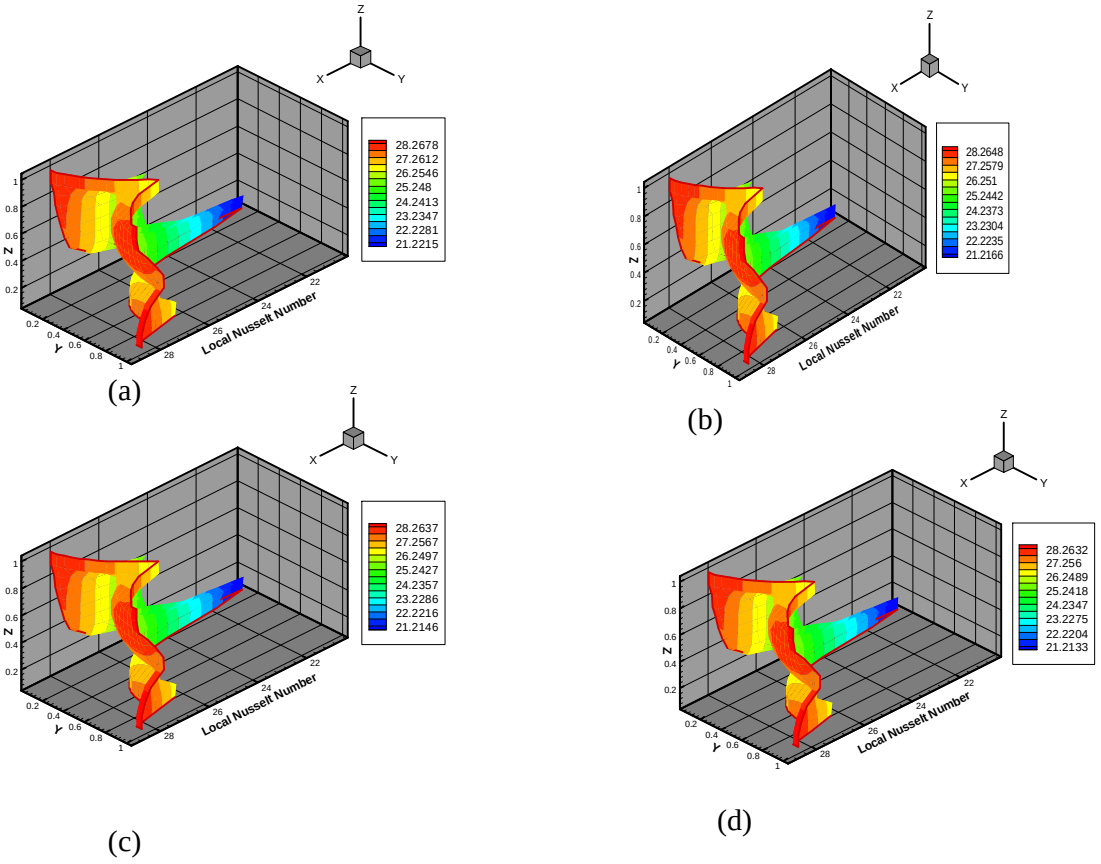


Figure (7) Local Nu contour for hot wall, Ω=50 rad/s : (a) $\Delta T = 100$ **,** **Ra=1.19**$*10^8$ **,** $Ra_r = 2.88*10^{10}$ **(b)** $\Delta T = 200$ **, Ra=2.09**$*10^8$ **,** $Ra_r = 5.08*10^{10}$ **(c)** $\Delta T = 300$ **, Ra=2.81**$*10^8$ **,** $Ra_r = 6.81*10^{10}$ **(d)** $\Delta T = 400$ **, Ra=3.39**$*10^8$ **,** $Ra_r = 8.21*10^{10}$ **.**

PDF created with pdfFactory Pro trial version www.pdffactory.com

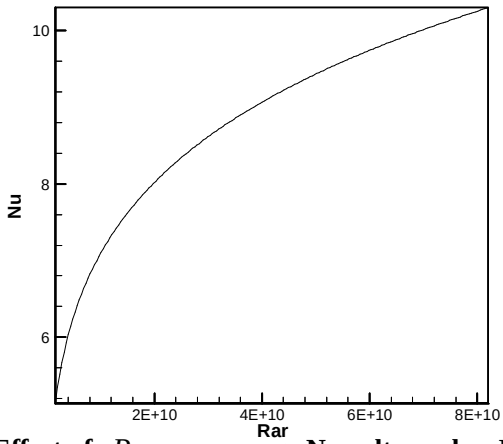


Figure (8) Effect of Ra_r on average Nusselt number Nu for different temperature difference ΔT and different angular velocities of enclosure Ω.

PDF created with pdfFactory Pro trial version www.pdffactory.com